A new flyback-current-fed push-pull DC-DC converter

2 authors, including:

Domingo Ruiz-Caballero
Pontificia Universidad Católica de Valparaíso
30 PUBLICATIONS   **316** CITATIONS

A New Flyback-Current-Fed Push–Pull DC–DC Converter

Domingo A. Ruiz-Caballero, *Student Member, IEEE,* and Ivo Barbi, *Senior Member, IEEE*

Abstract— This paper introduces a new flyback-current-fed push–pull dc–dc converter whose significant advantages in comparison with the conventional one are a reduction in the number of output diodes and unified output characteristics to represent both the buck and the boost operation modes in the continuous conduction mode. Theoretical analysis, design methodology, and experimental results taken from a 600-W 25-kHz laboratory prototype are presented in this paper. The circuit introduced is suitable for switching mode power supply design and power-factor-correction applications as well.

Index Terms— DC–DC converters, flyback converter, power supply, push–pull converter.

NOMENCLATURE

D	Duty ratio.
F_s	Switching frequency.
$\overline{I}_O$	Normalized average output current.
$\overline{I}_{L_{1P\min}}$	Normalized minimum current through L_{1P}.
$\overline{I}_{L_{1P\max}}$	Normalized maximum current through L_{1P}.
$\overline{I}_{L_{1S\min}}$	Normalized minimum current through L_{1S}.
$\overline{I}_{L_{1S\max}}$	Normalized maximum current through L_{1S}.
I_{L1P}	Current through L_{1P}.
I_{L1S}	Current through L_{1S}.
I_i	Average input current.
I_o	Average output current.
i_{S1}, i_{S2}	Current through switches S_1 and S_2.
$\overline{\Delta}i_{L_{1S}}$	Normalized ripple current through L_{1S}.
$\overline{\Delta}i_{L_{1P}}$	Normalized ripple current through L_{1P}.
N	Transformers turns ratio.
P_o	Output power.
V_{GS}	Gate–source MOSFET voltage.
V_{L2P}	Voltage across the push–pull primary winding.
$\overline{V}_o$	Normalized average output voltage.
V_o	Output voltage.
V_i	Input voltage.
V_{S1}, V_{S2}	Voltage across switches S_1 and S_2.
$V_{i\min}$	Minimum input voltage.
$V_{i\max}$	Maximum input voltage.
$\Delta V_{C_o}/V_o$	Normalized ripple output voltage.
ΔV_{Sw}	Saturation voltage across the switches.
η	Efficiency.
t	Time.

Δt_1	Time interval where for both buck and boost modes S_1 is turn on.
$\Delta t_1'$	Time interval where for both buck and boost modes a current flows through the flyback transformer.

I. INTRODUCTION

THE flyback-current-fed push–pull dc–dc converter [1], [2] has several advantages over the conventional voltage or current-fed push–pull ones. It has one single input and no output inductor, which makes it a good choice for a multiple output power supply. Besides, it provides inherent protection against transformer saturation. It is also recognized that this converter is more reliable than the conventional push–pull one due to the presence of the input inductor.

However, some disadvantages have been detected, namely, the existence of four diodes on the secondary side, and the impossibility of representing the operation for duty ratio from zero up to one, by the same set of output characteristics.

The circuit introduced in this paper is generated from the traditional flyback-current-fed push–pull topology, simply by removing diodes d_{03} and d_{04}, as shown in Fig. 1.

The new converter is composed of a push–pull transformer and one two-winding flyback transformer. In addition, the circuit includes two switches and two output diodes. The converter's characteristics are as follows.

1) It has two operation modes, namely, buck and boost that depend exclusively on the duty ratio. For duty ratio less than 0.5, it operates in the buck mode (nonoverlapping mode), and for duty ratio larger than 0.5, it operates in the boost mode (overlapping mode).
2) Its switches are at the same reference point, which simplifies the driving circuitry.
3) When both transformers have the same turns ratio, the output characteristics in continuous conduction mode (CCM) are the same for both the overlapping and the nonoverlapping operation modes.
4) It has only two output diodes.

The operation of the new circuit, represented in Fig. 1, is described in the following section.

II. PRINCIPLE OF OPERATION FOR $D < 0.5$

In order to simplify the analysis of the proposed converter, we assume that all passive and active components are ideal and $n_1/n_2 = n_3/n_4 = N$.
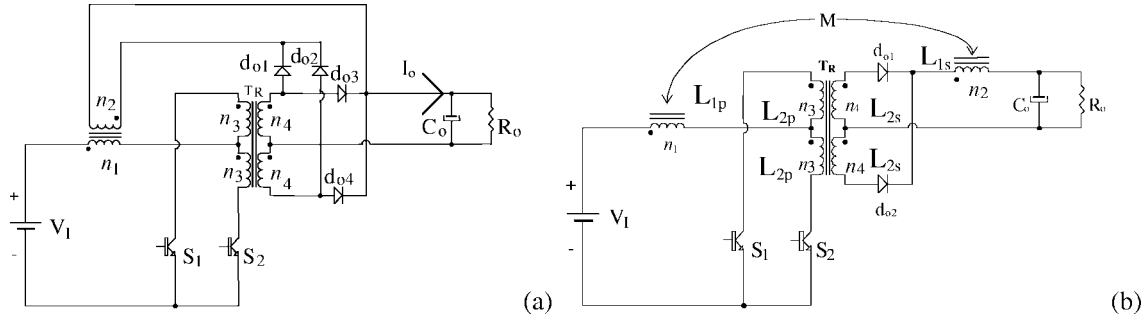
Fig. 1. (a) The conventional and (b) the new flyback-current-fed push–pull dc–dc converter.
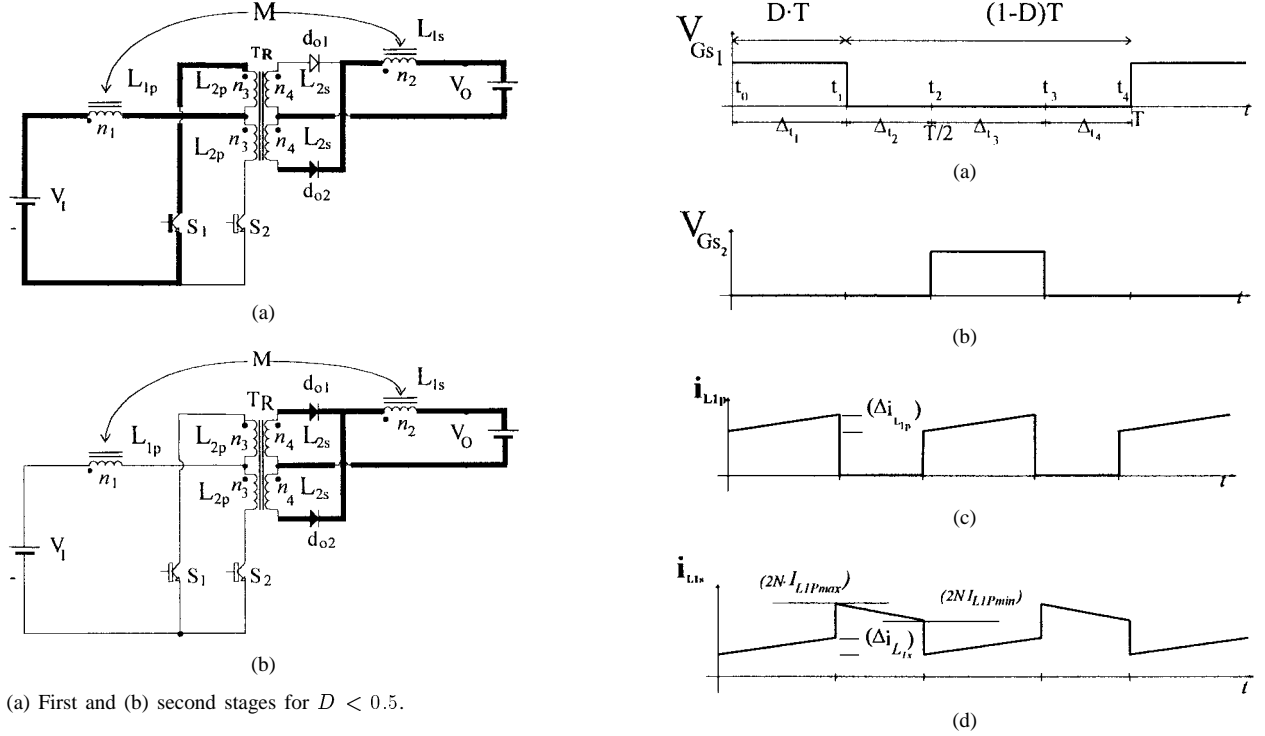

Fig. 2. (a) First and (b) second stages for $D < 0.5$.

In the buck mode, four topological states exist within a switching period. However, it is necessary to describe only two of them, as the remaining two stages are analogous.

The stages of operation for a half cycle are shown in Fig. 2. They are described as follows.

First Stage (t_0, t_1): At the instant $t = t_o$, S_1 turns on and a current flows through L_{1p}, L_{2p}, and S_1. The voltage across L_{2p} is reflected across the push–pull secondary windings (L_{2S}) and d_{o2} is turned on. The flyback transformer acts as an inductor, storing energy. The load receives energy only from the push–pull transformer. This stage exists for both the continuous and the discontinuous conduction modes.

Second Stage (t_1, t_2): At $t = t_1$, S_1 turns off and the flyback transformer transfers energy to the load with a current which is twice the current of the previous time interval. The value of the current flowing through each diode is equal to the current through the diode that was on during the previous time interval. Since both diodes are conducting, the push–pull transformer is short circuited. This stage ends when S_2 turns on.

In the discontinuous conduction mode (DCM), this stage ends when the inductor current reaches zero and then a
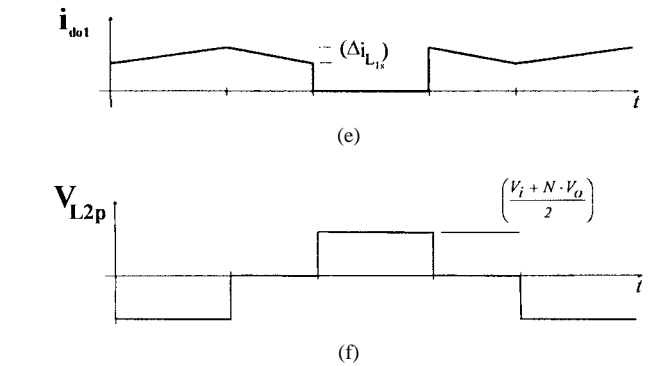

Fig. 3. Waveforms for the new converter working at $D < 0.5$ in CCM: (a) and (b) driving signals, (c) input current, (d) current through the inductor L_{1s}, (e) current through the output diodes, and (f) voltage across the primary winding of the push–pull transformer.

third stage can be observed, in which there is no transfer of energy. The load is supplied by the output capacitor. The corresponding theoretical waveforms for continuous and discontinuous current modes are shown in Figs. 3 and 4, respectively.
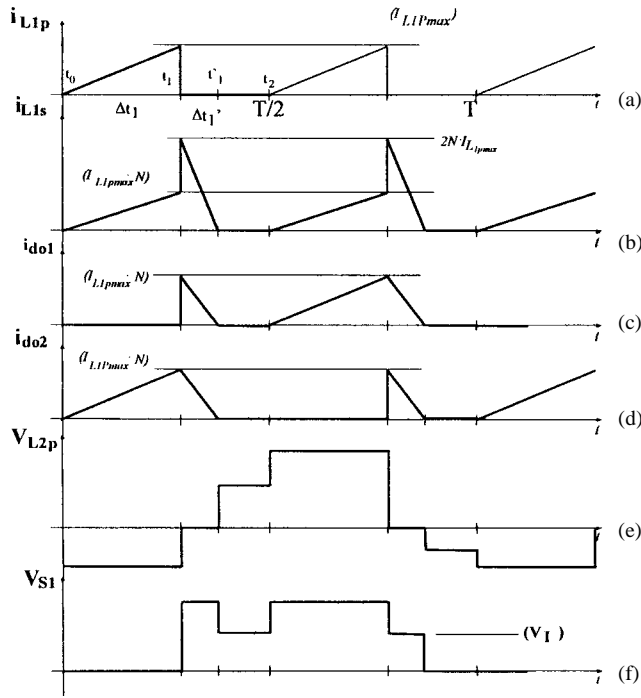
Fig. 4. Waveforms for discontinuous operation mode at $D < 0.5$: (a) current through the primary winding L_{1P}, (b) current through secondary winding L_{1S}, (c) and (d) current through output diodes, (e) voltage across the primary winding of the push–pull transformer, and (f) voltage across the switches.
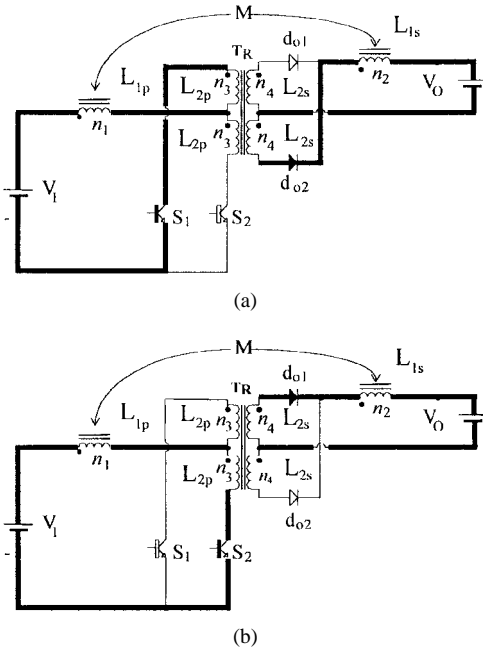

Fig. 5. (a) First and (b) second stages for $D = 0.5$.

III. PRINCIPLE OF OPERATION FOR $D = 0.5$

The stages of operation for $D = 0.5$ are shown in Fig. 5 and are described as follows.

First Stage (t_0, t_1): At the instant $t = t_o$, S_1 is turned on while S_2 is turned off, and a current flows through L_{1p}, L_{2p}, and S_1. The voltage across L_{2p} is reflected across the push–pull secondary windings (L_{2S}). The diode d_{o2} is turned
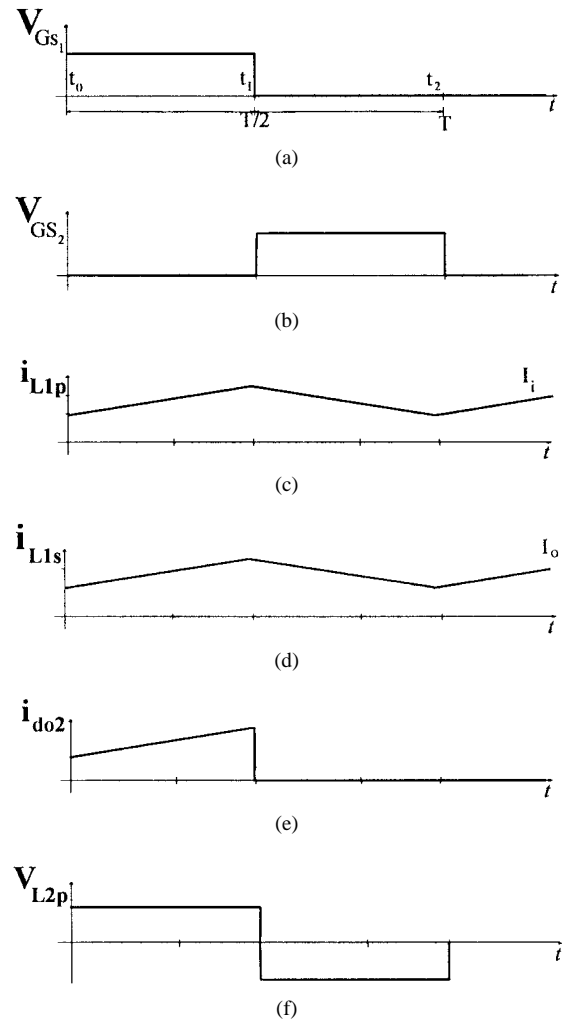

Fig. 6. Theoretical waveforms for the converter operating at $D = 0.5$: (a) and (b) driving signals of S_1 and S_2, (c) current through the primary winding L_{1P}, (d) current through the secondary winding L_{1S}, (e) current through output diodes, and (f) voltage across the primary winding of the push–pull transformer.

on. The flyback transformer does not transfer any power to the load, which is supplied only by the push–pull transformer.
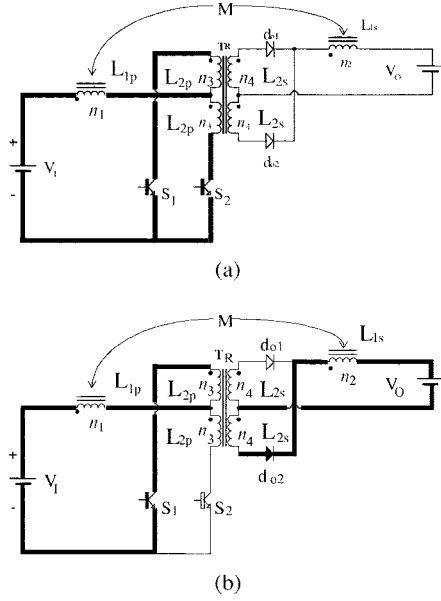
Second Stage (t_1, t_2): At the instant $t = t_1$, S_2 is turned on and S_1 is turned off. All electrical and magnetic variables evolve in a manner similar to the previous stage.

The principal features of the converter when operating at $D = 0.5$ is that it works like a continuous current electronic transformer and theoretically never operates in the discontinuous current mode. Theoretical waveforms are shown in Fig. 6.

IV. PRINCIPLE OF OPERATION FOR $D > 0.5$

The circuits representing the stages of operation for a half cycle are shown in Fig. 7.

First Stage (t_0, t_1): When this stage begins, switch S_2 is already on. At $t = t_o$, S_1 is gated on, conducting simultaneously with S_2. Diodes d_{o1}, d_{o2} are reverse biased. Current starts flowing through the push–pull primary windings L_{2P} so that the fluxes induced by the primary windings are in opposite

Fig. 7. (a) First and (b) second stages for $D > 0.5$.

directions, causing a magnetic short circuit in the transformer. As a result, energy is stored in L_{1P}.

Second Stage (t_1, t_2): At the instant $t = t_1$, S_2 is turned off and energy begins to be transferred to the load. This energy transfer occurs in two ways: directly through the push–pull transformer and indirectly through the flyback transformer (which delivers the energy stored during the previous time interval).

When operating in the discontinuous mode, the boost mode also presents a third stage, with no energy transfer, in which the load is supplied by the output capacitor. This interval finishes at $t = T/2$ when S_2 turns on.

The theoretical waveforms for CCM and DCM are shown in Figs. 8 and 9, respectively.

V. OUTPUT CHARACTERISTICS

The normalized load current is given by

$$\overline{I}_o = \frac{2 \cdot L_{1S} \cdot F_S \cdot N}{V_i} I_o. \quad (1)$$

The normalized load voltage is given by

$$\overline{V}_o = N \frac{V_o}{V_i}. \quad (2)$$

The transformers turns ratio are given by

$$N = \frac{n_1}{n_2} = \frac{n_3}{n_4}. \quad (3)$$

The output characteristics in the continuous current mode for any duty ratio are given by

$$\overline{V}_o = \frac{D}{(1-D)}. \quad (4)$$

In DCM the output characteristics are represented by two different expressions. For the buck mode, they are given by

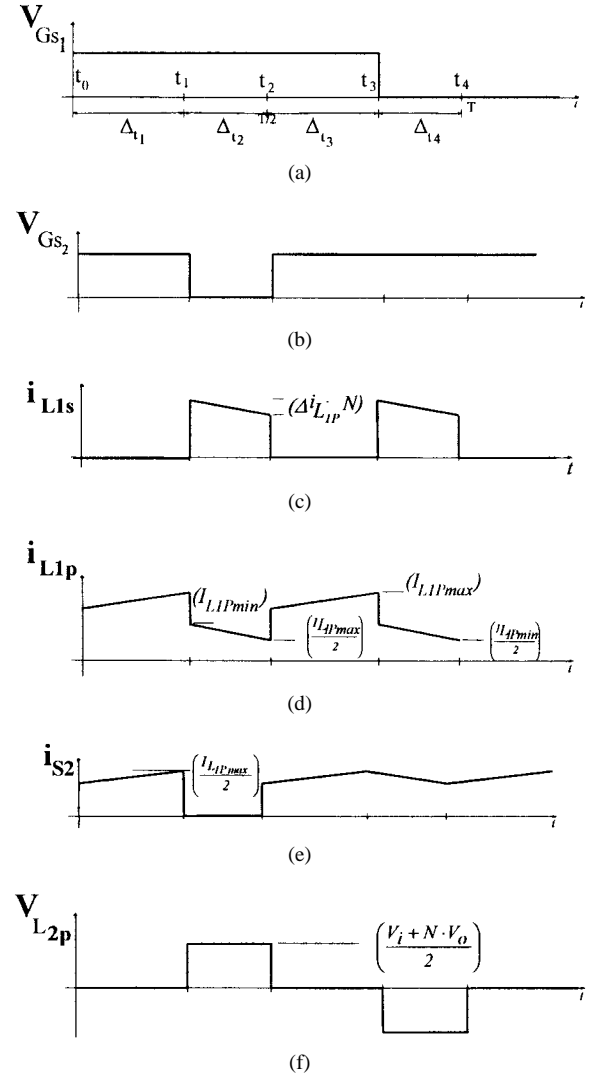$$\overline{V}_o = \frac{D^2}{(2 \cdot \overline{I}_o + D^2)}. \quad (5)$$

Fig. 8. Waveforms for the converter operating at $D > 0.5$ in CCM: (a) and (b) driving signals of S_1 and S_2, (c) current through the secondary winding L_{1S}, (d) current through the primary winding L_{1P}, (e) current through the switches, and (f) voltage across the primary winding of the push–pull transformer.

The boundary between DCM and CCM for $D < 0.5$ is given by

$$\overline{V}_o = \frac{1 - 4 \cdot \overline{I}_o - \sqrt{1 - 16 \cdot \overline{I}_o}}{2 \cdot (2 \cdot \overline{I}_o + 1)}. \quad (6)$$

For the boost mode, the output characteristics in DCM are given by

$$\overline{V}_o = \frac{(2 \cdot D - 1)^2 + 2 \cdot \overline{I}_o}{2 \cdot \overline{I}_o}. \quad (7)$$

The boundary between DCM and CCM for $D > 0.5$ is given by

$$\overline{I}_o = \frac{[\overline{V}_o - 1]}{2 \cdot [1 + \overline{V}_o]^2}. \quad (8)$$

The unified output characteristics of the converter are shown in Fig. 10. They are created by the superposition of the
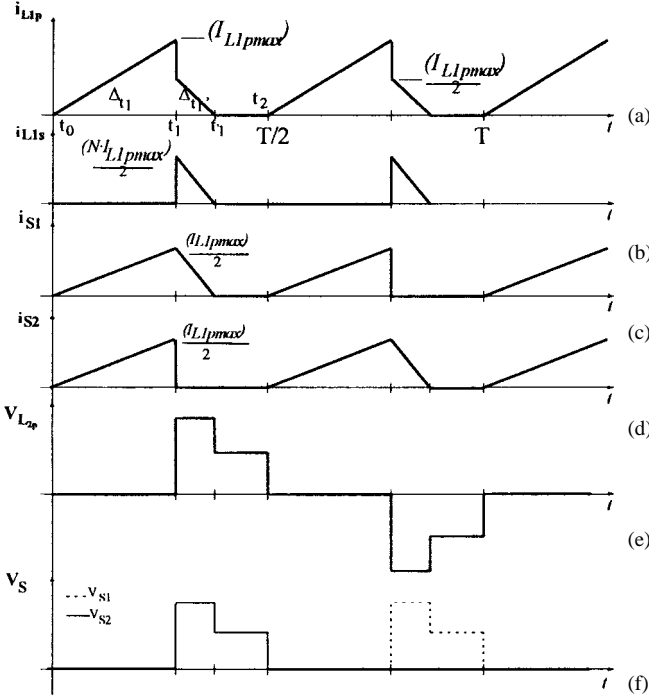
Fig. 9. Waveforms for the discontinuous conduction mode and $D > 0.5$: (a) current through the primary winding L_{1P}, (b) current through secondary winding L_{1S}, (c) current through switch S_1, (d) current through switch S_2, (e) voltage across the primary winding of the push–pull transformer L_{2p}, and (f) voltage across the switches.
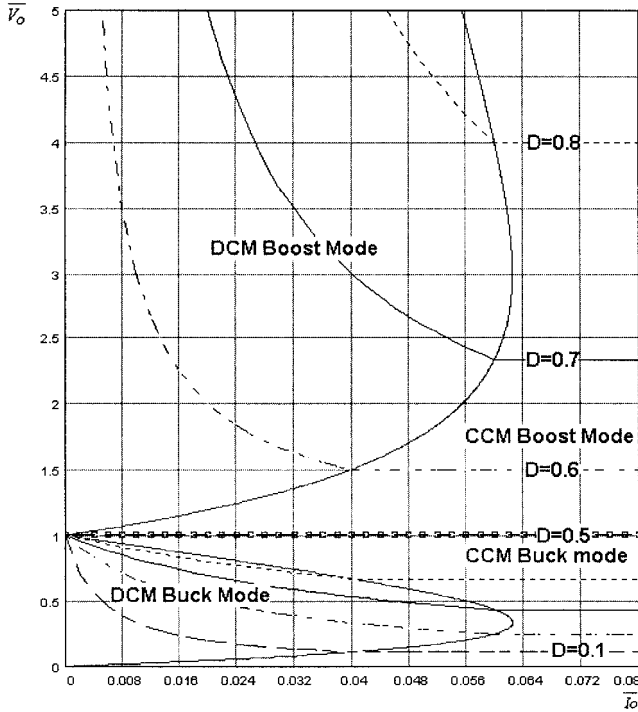

Fig. 10. Unified output characteristics.

individual output characteristics of the classic buck and boost converters.

For $D = 0.5$ the converter will never operate in the discontinuous conduction mode, even for light loads.
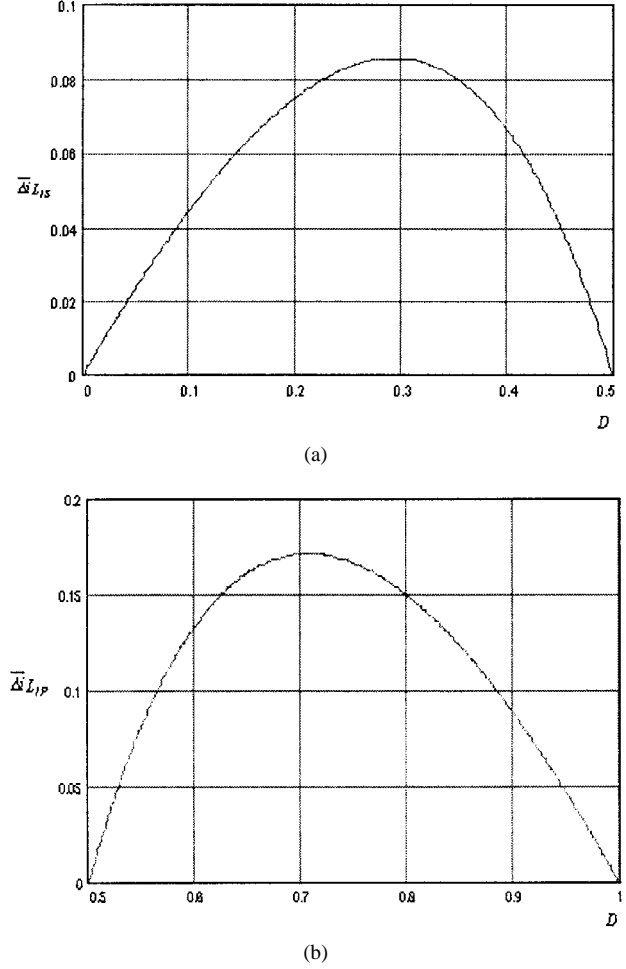

(a)

(b)

Fig. 11. (a) Current ripple for buck and (b) boost modes as function of D.

The normalized minimum load current which ensures continuous current mode is $\overline{I_{o\,\min}} = 0.0625$ for both the buck and the boost modes.

VI. INPUT AND OUTPUT CURRENT RIPPLE

For $D < 0.5$, according to the waveforms shown in Fig. 3, the normalized output current ripple is given by

$$\overline{\Delta}i_{L1S} = \overline{I}_{L1S_{\max}} - \overline{I}_{L1S_{\min}}. \tag{9}$$

$\overline{\Delta}i_{L1S}$, $\overline{I}_{L1S_{\max}}$, and $\overline{I}_{L1S_{\min}}$ are given by

$$\overline{\Delta}i_{L1S} = \frac{2 \cdot L_{1S} \cdot F_S \cdot N}{V_i} \cdot \Delta i_{L1S} \tag{10}$$

$$\overline{I}_{L1S_{\max}} = \frac{\overline{I}_o}{(1-D)} + \frac{D \cdot (1 - 2 \cdot D)}{4 \cdot (1-D)} \tag{11}$$

$$\overline{I}_{L1s_{\min}} = \frac{\overline{I}_o}{(1-D)} - \frac{D \cdot (1 - 2 \cdot D)}{4 \cdot (1-D)}. \tag{12}$$

By substituting (11) and (12) into (9), one obtains (13)

$$\overline{\Delta}i_{L1S} = \frac{(1 - 2 \cdot D) \cdot D}{2 \cdot (1-D) \cdot)}. \tag{13}$$

For $D > 0.5$, according to the waveforms shown in Fig. 8, the normalized input current ripple is given by

$$\overline{\Delta}i_{L1P} = \overline{I}_{L1P_{\max}} - \overline{I}_{L1P_{\min}}. \tag{14}$$
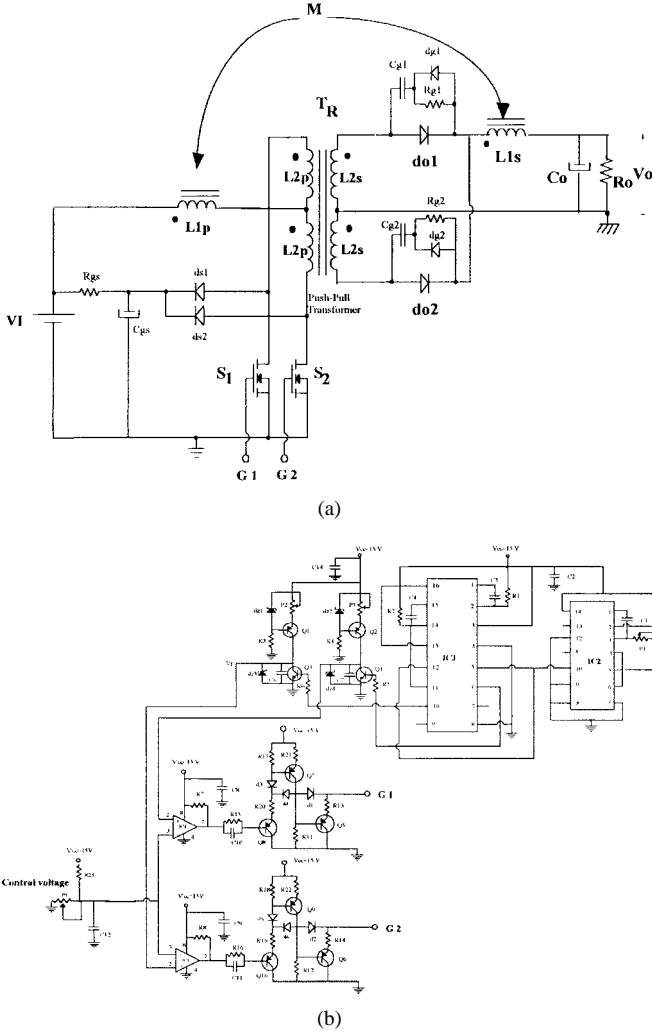
Fig. 12. (a) Power stage and (b) control circuit diagram.

$\overline{\Delta}i_{L_1P}$, $\overline{I}_{L_1P_{\max}}$, and $\overline{I}_{L_1P_{\min}}$ are given by

$$\overline{\Delta}i_{L_1P} = \frac{2 \cdot L_{1P} \cdot F_S \cdot N}{V_o} \cdot \Delta i_{L_1P} \qquad (15)$$

$$\overline{I}_{L_1P_{\max}} = \frac{\overline{I}_i}{D} + \frac{(2 \cdot D - 1) \cdot (1 - D)}{2 \cdot D} \qquad (16)$$

$$\overline{I}_{L_1P_{\min}} = \frac{\overline{I}_i}{D} - \frac{(2 \cdot D - 1) \cdot (1 - D)}{2 \cdot D}. \qquad (17)$$

By substituting (16) and (17) into (14), one obtains

$$\overline{\Delta}i_{L_1P} = \frac{(2 \cdot D - 1) \cdot (1 - D)}{D}. \qquad (18)$$

Expressions (13) and (18) are represented in Fig. 11(a) and (b), respectively.

The ripple currents $\overline{\Delta}i_{L_1P}$ and $\overline{\Delta}i_{L_1S}$ are similar to the primary and secondary flyback transformer ripple currents of the conventional push–pull converter.

VII. EXPERIMENTAL RESULTS

A laboratory prototype, operating in the continuous conduction mode, has been designed and implemented. Its specifica-

(a)

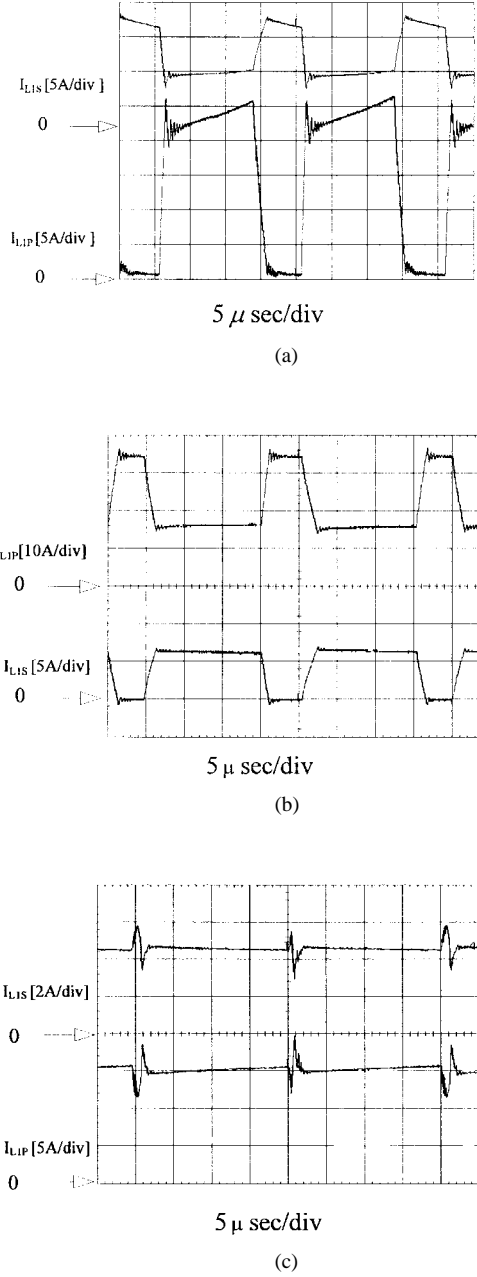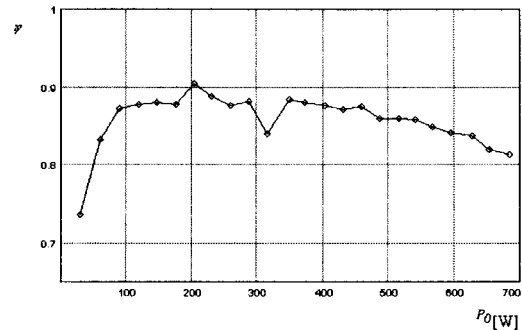5 μ sec/div

(b)

5 μ sec/div

(c)

Fig. 13. Experimentally obtained input (I_{L1P}) and output (I_{L1S}) currents for (a) $D = 0.3$, (b) $D = 0.6$, and (c) $D = 0.5$.

Fig. 14. Experimentally obtained efficiency as a function of the converter output power in the buck mode.
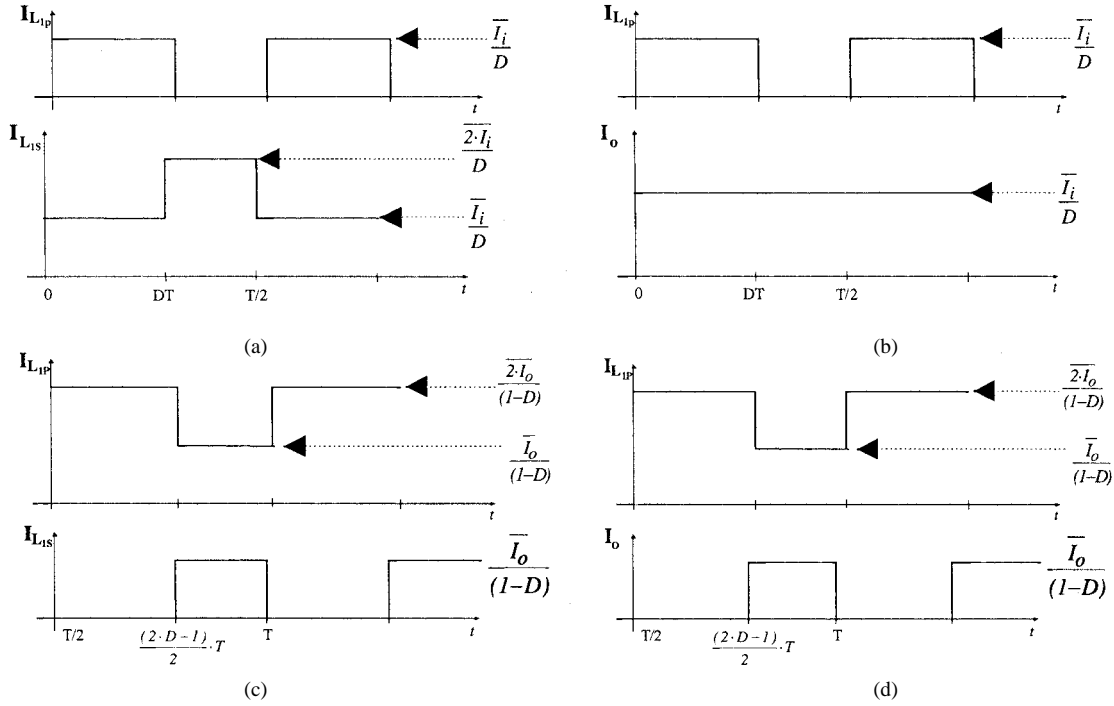
Fig. 15. Input and output currents with $L_{1p} = L_{1S} = \infty$ and $N_1 = N_2 = 1$: (a) new converter with $D < 0.5$, (b) $D > 0.5$, (c) the conventional converter with $D < 0.5$, and (d) $D > 0.5$.

TABLE I
POWER STAGE COMPONENTS

S_1, S_2	IRFP150
do_1, do_2	MUR 135
dg_1, dg_2	SKE 4f2/04
Cg_1, Cg_2	4700pF, 1.6kV polypropylene
Rg_1, Rg_2	47k Ω, 1/2W
Co	1000uF, 250V
C_{gs}	100uF
d_{S1}, d_{S2}	MUR 1530
R_{gS}	60 Ω
Flyback transformer: core E-65/26, N=0.33, airgap: 0.5mm,	n_1=9 turns, AWG 22, 13 wires, n_2=27 turns, AWG 22, 8wires.
T_R: core E-65/26, N=0.33.	n_3=n_5=6 turns, AWG 22, 9 wires, n_4=n_6=18 turns, AWG 22, 5 wires.

TABLE II
CONTROL CIRCUIT COMPONENTS

P1	56 k Ω
P2,P3	1 k Ω
P4	10 k Ω
R_1, R_2	5.6 k Ω, 1/8W
R_3, R_4	15 k Ω, 1/8W
R_5, R_6	100 Ω, 1/8W
R_7, R_8	1 k Ω, 1/8W
R_9, R_{10}	15 k Ω, 1/4W
R_{11}, R_{12}	1 k Ω, 1/4W
R_{13}, R_{14}	15 k Ω, 1/4W
$R_{15}, R_{16}, R_{17}, R_{18}$	1 k Ω, 1/4W
R_{19}, R_{20}	2.2 k Ω, 1/4W
R_{21}, R_{22}	6.8 Ω, 1/4W
R_{23}	20 k Ω, 1/4W
C_1	82 pF
C_2	100 nF
C_3, C_4	27 pF
C_5, C_6, C_7	56 nF
C_8, C_9	100 nF
C_{10}, C_{11}	1 nF
C_{12}	1.2 nF
$d_1, d_2, d_3, d_4, d_5, d_6$	1N4148
dz_1, dz_2	2.7V 1N4371
dz_3, dz_4	5.1V 1N751
Q_1, Q_2	BC558B, PNP
Q_3, Q_4	BC537, NPN
$Q_5, Q_6, Q_7, Q_8, Q_9, Q_{10}$	BC327, PNP
IC_1	LM311
IC_2	CD4047BE
IC_3	CD4528BE

tions are as follows:

$$P_o = 600 \text{ W} \qquad V_{i_{\max}} = 48 \text{ V} \qquad V_{i_{\min}} = 15 \text{ V}$$

$$F_S = 25 \text{ kHz} \qquad V_o = 60 \text{ V} \qquad I_o = 10 \text{ A}$$

$$\frac{\Delta V_{co}}{V_o} = 0.01 \qquad \Delta i_{L_{1S}} = 1 \text{ A} \qquad \Delta V_{SW} = 1 \text{ V}.$$

The turns ratio N is calculated by using $D = 0.3$, which is the duty ratio that causes the maximum output current ripple in the buck mode. With the saturation voltage across the switches equal to 1 V, from (2), we obtain $N = 0.33$.

TABLE III
COMPARISON BETWEEN THE NEW AND THE CLASSIC CONVERTER

RELATIONSHIPS	NEW FLYBACK PUSH PULL		CLASSIC FLYBACK PUSH PULL	
RMS input current	$i_i = \dfrac{\sqrt{2 \cdot D}}{2 \cdot N \cdot (1-D)}$	16.17A	$i_i = \dfrac{\sqrt{2 \cdot D}}{N}$, $\quad$ (D<0.5)	16.13A
Voltage across the switches.	$\dfrac{V_S}{V_i} = \dfrac{1}{(1-D)}$	68.57V	$\dfrac{V_S}{V_i} = 1 + 2 \cdot D$, $\quad$ (D<0.5) $\dfrac{V_S}{V_i} = \dfrac{1}{(1-D)}$, $\quad$ (D>0.5)	76.8V
Average current through the switches.	$\dfrac{I_{SW}}{I_o} = \dfrac{D}{2 \cdot N \cdot (1-D)}$	6.26A	$\dfrac{I_{SW}}{I_o} = \dfrac{D}{N}$, $\quad$ (D<0.5) $\dfrac{I_{SW}}{I_o} = \dfrac{D}{2 \cdot N \cdot (1-D)}$, $\quad$ (D>0.5)	6.25A
RMS current through the switches.	$\dfrac{I_{SW}}{I_o} = \dfrac{\sqrt{D}}{2 \cdot N \cdot (1-D)}$	11.439A	$\dfrac{I_{SW}}{I_o} = \dfrac{\sqrt{D}}{N}$, $\quad$ (D<0.5) $\dfrac{I_{SW}}{I_o} = \dfrac{\sqrt{D}}{2 \cdot N \cdot (1-D)}$, $\quad$ (D>0.5)	11.41A
Flyback transformer turns-ratio.	$N = \dfrac{D}{\frac{V_o}{V_i} \cdot (1-D)}$	0.342	$N = \dfrac{2 \cdot D}{\frac{V_o}{V_i}}$, $\quad$ (D<0.5) $N = \dfrac{D}{\frac{V_o}{V_i} \cdot (1-D)}$, $\quad$ (D>0.5)	0.48
Push-pull transformer turns-ratio.	$N = \dfrac{D}{\frac{V_o}{V_i} \cdot (1-D)}$	0.342	$N = \dfrac{2 \cdot D}{\frac{V_o}{V_i}}$, $\quad$ (D<0.5) $N = \dfrac{D}{\frac{V_o}{V_i} \cdot (1-D)}$, $\quad$ (D>0.5)	0.48
RMS current through the output capacitor.	$I_{Co} = \sqrt{\dfrac{2 - 3 \cdot D}{2 \cdot (1-D)^2} - 1} \cdot I_o$ (D<0.5) $I_{Co} = \sqrt{\dfrac{1 - 4 \cdot D \cdot (1-D)}{(1-D)}} \cdot I_o$ (D>0.5)	5.05A	Zero, $\quad$ (D<0.5) $I_{Co} = \sqrt{\dfrac{1 - 4 \cdot D \cdot (1-D)}{(1-D)}} \cdot I_o$, (D>0.5)	0

The primary and secondary flyback transformer inductances L_{1p} and L_{1s} are calculated using (10) and (13). The values obtained are $L_{1S} = 249.312$ μH and $L_{1P} = 27.15$ μH.

The duty ratio for $V_{i\,\min}$ and $V_{i\,\max}$, calculated using (2) and (4), is as follows:

$$D_{\min} = 0.3, \qquad \text{for } V_{i\,\max} = 48 \text{ V}$$

and

$$D_{\max} = 0.6, \qquad \text{for } V_{i\,\min} = 15 \text{ V}.$$

The power and control diagrams are shown in Fig. 12 and the parameters of the prototype are given in Tables I and II for the power stage and the control circuit, respectively.

We have added a clamping circuit composed of d_{s1}, d_{s2}, C_{gs}, and R_{gs} to prevent overvoltages across of switches, caused by the leakage inductance in the transformers.

Fig. 13(a) shows the input (I_{L1P}) and the output currents (I_{L1S}) for $D = 0.3$ at rated load power, which is equal to 600 W. Fig. 13(b) shows the input (I_{L1P}) and the output current (I_{L1S}) for $D = 0.6$. Finally, Fig. 13(c) shows the

input (I_{L1P}) and the output currents (I_{L1S}) for $D = 0.5$. The waveforms shown in Fig. 13(b) and (c) were taken at output power equal to 300 W.

The experimental waveforms confirm that for $D = 0.5$, both the output and the input currents are ripple free, which characterizes the behavior of an ideal dc–dc transformer.

Fig. 14 shows the experimentally obtained efficiency of the implemented converter, utilizing a dissipative clamping circuit, for $V_0 = 60$ V and $V_i = 48$ V.

VIII. COMPARISON BETWEEN THE PROPOSED AND THE CONVENTIONAL FLYBACK-CURRENT-FED PUSH–PULL CONVERTER

Let us compare the waveforms of the input and output currents of both converters, taking $N = 1$, and very large inductances L_{1p} and L_{1s}. These currents are represented in Fig. 15(a) and (b) for the new converter and in Fig. 15(c) and (d) for the conventional one. We note that for $D > 0.5$, operation in the boost mode, both converters behave identically. For $D < 0.5$, when operating in the buck mode,

the output current of the new converter is composed of two steps, while the same current in the conventional converter is constant. Therefore, the new converter requires a larger output filter capacitor.

These disadvantages do not exist when $N \neq 1$, situation where both converters operate with pulsed output current.

Table III shows the most relevant equation describing the behavior of both converters and numerical values generated by these equation for $V_i = 48$ V, $V_o = 60$ V, $D = 0.3$, and $I_o = 10$ A.

Details about the deduction of these equations can be found in [3].

IX. CONCLUSIONS

From our study, as reported in this paper, we draw the following conclusions.

- The new converter preserves all the basic properties of the conventional flyback current-fed push–pull converter with fewer components.
- It operates in both buck and boost modes, which are represented by the same mathematical model.
- It is the opinion of the authors that the introduced converter is suitable for switching mode power supplies design and power-factor-correction applications, with advantage over the classic push–pull dc–dc converter.

REFERENCES

[1] V. J. Thottuvelil, T. G. Wilson, and H. A. Owen, Jr., "Analysis and design of a push–pull current-fed converter," in *IEEE Power Electronic Specialist Conf., 1981 Rec.,* pp. 192–203.

[2] R. Redl and N. Sokal, "Push–pull current-fed, multiple output regulated wide input range dc/dc power converter with only one inductor and with 0 to 100% switch duty ratio: Operation at duty ratio below 50%," in *IEEE Power Electronic Specialist Conf., 1981 Rec.,* pp. 204–212.

[3] D. A. Ruiz-Caballero, "A new flyback-push–pull current-fed dc to dc converter: Theoretical and experimental development," Ph.D. dissertation, Federal Univ. Santa Catarina, Brazil, 1999 (in Portuguese).

Domingo A. Ruiz-Caballero (S'97) was born in Santiago, Chile, in 1963. He received the degree in electrical engineering from the Universidad Católica de Valparaíso, Valparaíso, Chile, in 1989 and the M.Eng. degree from the Federal University of Santa Catarina, Florianópolis, Santa Catarina, Brazil, in 1992. He is currently working towards the Dr.Eng. degree at the Federal University of Santa Catarina.

His interests include dc/dc converters, power-factor-correction techniques, and soft-switching techniques.

Ivo Barbi (M'78–SM'90) was born in Gaspar, Santa Catarina, Brazil, in 1949. He received the B.S. and M.S. degrees in electrical engineering from the Federal University of Santa Catarina, Florianópolis, Brazil, in 1973 and 1976, respectively, and the Ph.D. degree from the Institut National Polytechnique de Toulouse, France, in 1979.

He founded the Brazilian Power Electronics Society and the Power Electronics Institute of the Federal University of Santa Catarina. Currently, he is a Professor of the Power Electronics Institute. Dr. Barbi has been an Associate Editor in the Power Converters Area for the IEEE TRANSACTIONS ON INDUSTRIAL ELECTRONICS since January 1992.